Differential expression profiles of miRNA in granulomatous lobular mastitis and identification of possible biomarkers

JIE LING[1], XIANMIN XIE[2], YUE WANG[3], WEIFANG HUANG[1], JUN LUO[1], JINGQUN SU[1], HONGQIAO FAN[3], SHITING WU[3] and LIFANG LIU[3]

[1]Graduate School, Hunan University of Chinese Medicine; Departments of [2]Hand Surgery and [3]Galactophore, The First Hospital of Hunan University of Chinese Medicine, Changsha, Hunan 41000, P.R. China

Abstract. The etiology and pathogenesis of granulomatous lobular mastitis (GLM) remain largely elusive and the expression levels and regulatory roles of microRNAs (miRNAs or miRs) in GLM have remained mostly undetermined. In the present study, the miRNAs that were differentially expressed in breast biopsy samples from patients with GLM and normal tissue adjacent to fibroadenoma were analyzed, a comprehensive differential expression profile of miRNAs was provided and potential biomarkers were screened out. The expression profile of miRNAs was determined by high-throughput sequencing in the tissues of patients with GLM and healthy controls. Significantly differentially expressed miRNAs were screened by threshold setting and cluster analysis and their target genes were analyzed by Gene Ontology (GO) and Kyoto Encyclopedia of Genes and Genomes (KEGG) enrichment. Finally, circulating differentially expressed miRNAs between the GLM and control groups were further analyzed by reverse transcription-quantitative PCR (RT-qPCR). A total of 31,077 miRNAs were detected by high-throughput sequencing. By using the cutoff criteria of |log2 fold change|>2.5 and q<0.001, 13 miRNAs that were indicated to be GLM biomarkers were screened out. The expression levels of these 13 miRNAs in the GLM group were higher than those in the control group. GO and KEGG enrichment analyses suggested that the occurrence and development of GLM may be associated with autoimmune inflammation, metabolism and pathogenic organisms. miR-451a and miR-5571-3p were confirmed to be significantly increased in the serum of patients with GLM compared with their levels in the serum of healthy volunteers, which suggests that they may be used as biomarkers of GLM. To the best of our knowledge, the present study was the first report detailing genome-wide miRNA profiling of patients with GLM compared with controls. The possible targets and pathways of GLM were evaluated by bioinformatics analysis. The present study identified 13 differentially expressed miRNAs with important theoretical significance and potential application. Furthermore, miR-451a and miR-5571-3p were verified by RT-qPCR as possible biomarkers of GLM.

Introduction

Granulomatous lobular mastitis (GLM), also known as granulomatous mastitis (GM) or idiopathic GM (IGM), tends to occur in females of childbearing age with a history of breastfeeding and childbearing (1). The main manifestations of GLM are palpable breast lumps, swelling and pain on one or both sides of the breast, which may be accompanied by skin blushes, inversion of the nipple, mammary duct fistula, arthritis and fever (2). Radiological examination of GLM is not specific and it may be easily confused with breast cancer (BC) (3). Pathological examination is the gold standard for GLM diagnosis. The possible etiology includes autoimmune-related conditions (4,5), bacterial infection (6,7) and hyperprolactinemia (8). However, the etiology and mechanism of GLM remain controversial.

MicroRNAs (miRNAs or miRs) are a group of noncoding RNAs with ~22 nucleotides in length that are involved in the regulation of gene transcription and translation. These molecules work through binding to the untranslated region of mRNA, resulting in the inhibition of protein translation and possibly the destruction of the mRNA (9). Destruction of mRNA and errors in protein translation may lead to pathological changes in the human body. miRNAs may form stable complexes with proteins in peripheral blood and body fluids and these complexes may be used as biomarkers for disease diagnosis, disease evaluation and targeted therapy. Previous studies have demonstrated that miRNAs may be used as biomarkers for the diagnosis of multiple inflammatory diseases (10,11), severity judgment, prognosis assessment and therapeutic targets in the clinic. In GLM, a disease that requires an invasive diagnosis, the identification

Correspondence to: Dr Lifang Liu or Dr Shiting Wu, Department of Galactophore, The First Hospital of Hunan University of Chinese Medicine, 95 Shaoshan Middle Street, Changsha, Hunan 41000, P.R. China
E-mail: liulff@126.com
E-mail: 282379223@qq.com

of non-invasive diagnostic biomarkers may spare patients from pain during treatment and improve the treatment evaluation. Previous reports on GLM mostly focused on clinical treatment, retrospective analysis, detection of inflammatory indicators and epidemiological investigation. For instance, Aksan *et al* (12) verified that serum miR-21 and phosphatase and tensin homolog may serve as non-invasive biomarkers to help distinguish GLM from BC. To identify the regulatory mechanism and possible biomarkers associated with GLM, gene sequencing and clinical serum sample validation experiments were performed in the present study.

To date, there have been no reports on differential expression profile analysis of miRNA in GLM and normal tissues, to the best of our knowledge. Thus, in the present study, differentially expressed miRNAs were identified from GLM tissues and normal tissues located next to the fibroadenoma by high-throughput sequencing. Next, bioinformatics was used to analyze the signaling pathways in which the differentially expressed miRNAs were enriched. The expression of selected miRNAs was then verified in clinical serum samples. The present findings may serve as a basis for further research on mechanisms in GLM and demonstrated that high-throughput sequencing is a reliable method to study diseases with an unknown mechanism.

Materials and methods

Patients. The present study was approved by the Ethics Committee of The First Hospital of the Hunan University of Chinese Medicine (approval no. HN-LL-ZFKY-2019-004-01) and was performed in accordance with the Declaration of Helsinki. Written informed consent was obtained from all volunteers, comprising 10 patients diagnosed with GLM and 10 volunteers with fibroadenoma, and these two groups had the same demographic characteristics. The clinicopathological characteristics of the GLM cohort were a large amount of inflammatory cell infiltrate, granuloma formation and an age range of 30-44 years. The clinicopathological characteristics of the controls were acinus or ducts composed of epithelium and muscular epithelium, with loose structural hyperplasia surrounding the basement membrane, and their age was 25-46 years. All tissue samples were collected at The First Hospital of Hunan University of Chinese Medicine (Changsha, China) between June 2019 and July 2020. Serum samples were collected between December 2021 and April 2022 (the recruitment period was from July 2021 to July 2022; ethical approval no. HN-LL-KY-2021-020-01).

Normal tissue from volunteers was obtained from the tissue adjacent to their fibroadenoma during breast fibromectomy. Volunteers who had received any medications within 3 months and those with a history of immunopathology (such as type 1 diabetes, rheumatoid arthritis or psoriasis, as well as renal or cardiovascular disorders) or those who were pregnant or lactating were excluded from the study.

The GLM tissue was obtained by lesion excision after pathological diagnosis of GM. According to the aforementioned exclusion criteria, patients who had received glucocorticoid, immunosuppressor or antituberculosis drugs were excluded from the study.

An RNAlater protective solution (Beijing Applygen Gene Technology, Ltd.) was added to all tissues within 3 min of collection and the samples were preserved in liquid nitrogen.

Research method. Demographic data (including age, body weight and height, as well as body mass index), chief complaints, medical history, blood routine examination, biochemical parameters and pathology reports were obtained from the subjects' medical records (Table I).

RNA quantification and qualification. The tissue sample (150 mg) was placed in a tube at room temperature (20˚C) and 1.5 ml TRIzol® (Thermo Fisher Scientific, Inc.) was immediately added. The tubes were placed in a TissueLyser II (QIAGEN China Co., Ltd.) and lysed for 2 min at 20-30 Hz. After reassembling the adapter set, the TissueLyser was operated for another 2 min at 20-30 Hz. Following centrifugation at 12,000 x g for 5 min at 4˚C, the supernatant was collected to extract and purify the total RNA from the sample. Total RNA was evaluated as follows: RNA degradation and contamination was monitored on 1% agarose gels; RNA purity was assessed using a NanoPhotometer® spectrophotometer (Implen); the RNA concentration was calculated using a Qubit® RNA Assay Kit on a Qubit® 2.0 Fluorometer (Thermo Fisher Scientific, Inc.); and RNA integrity was assessed using the RNA Nano 6000 Assay Kit of the Agilent Bioanalyzer 2100 system (Agilent Technologies, Inc.).

Library preparation for small RNA sequencing. Sequencing libraries were generated using the small RNA samples. A total of 3 µg total RNA per sample was used as input material for the small RNA library. The Illumina DNA PCR-Free Library Prep Kit (New England BioLabs, Inc.) was used following the manufacturer's instructions. Using the special structure of the 3' and 5' ends of the small RNA (namely, the 5'end has a complete phosphate group, while the 3' end has a hydroxyl group) and using total RNA as the starting sample, the two ends of the small RNA were directly added to the adaptor and the cDNA was then synthesized by reverse transcription (RT) (Fig. 1). Once the library was constructed, Qubit2.0 (Thermo Fisher Scientific, Inc.) was used to preliminarily quantify the cDNA. Finally, the library quality was assessed with the Agilent Bioanalyzer 2100 system (Agilent Technologies, Inc.).

Clustering, sequencing and quality control. Clustering of the index-coded samples was performed on a cBot Cluster Generation System using the TruSeq SR Cluster Kit v3-cBot-HS (Illumina, Inc.) according to the manufacturer's instructions. Following cluster generation, the library preparations were sequenced on an Illumina HiSeq 2500/2000 platform. Raw data (raw reads) in the FASTQ format were first processed. In this step, clean data (clean reads) were obtained by removing from the raw data reads that contained poly-N (N>10%, since reads with >10% base information could not be identified), with 5' adapter contaminants or without 3' adapter or the insert tag, containing poly A, T, G or C, and low-quality reads (reads with a Phred quality Score ≤20 accounting for >30% of the total reads). At the same time, the Q20, Q30 and the GC-content of the raw data were calculated. A 18-35-nucleotide length was selected from the clean reads for downstream analyses.

Table I. Demographic characteristics and laboratory findings of GLM and control groups.

Parameter	GLM (n=10)	Control (n=10)	Normal ranges/limits	P-value
Age, years	34.20±4.94	35.30±7.02	-	0.796
BMI, kg/m^2	23.75±2.46	22.49±3.16	18.5-23.9	0.334
Glucose, mmol/l	5.46±1.48	4.84±0.61	3.89-6.11	0.481
Urea, mmol/l	4.04±1.04	4.06±0.96	2.14-7.14	0.965
Creatinine, μmol/l	59.00±5.46	56.80±8.15	45-84	0.487
AST, IU/l	18.29±3.99	16.15±3.59	0-32	0.223
ALT, IU/l	14.21±3.04	14.15±4.37	0-33	0.972
Albumin, g/l	47.78±5.38	46.40±4.44	35-52	0.540
Total protein, g/l	68.85±5.72	71.06±6.97	60-83	0.434
WBC, x10^9/l	12.83±3.25	6.76±2.57	3.5-9.5	<0.001
Hb, g/l	126.30±9.42	123.20±10.57	115-150	0.497
PLT, x10^9/l	254.50±57.48	242.60±80.34	125-350	0.708
INR	0.93±0.06	0.96±0.07	0.8-1.24	0.853

BMI, body mass index; AST, glutamic oxalacetic transaminase; ALT, glutamic-pyruvic transaminase; WBC, white blood cell; Hb, hemoglobin; PLT, platelets; INR, international normalized ratio; GLM, granulomatous lobular mastitis.
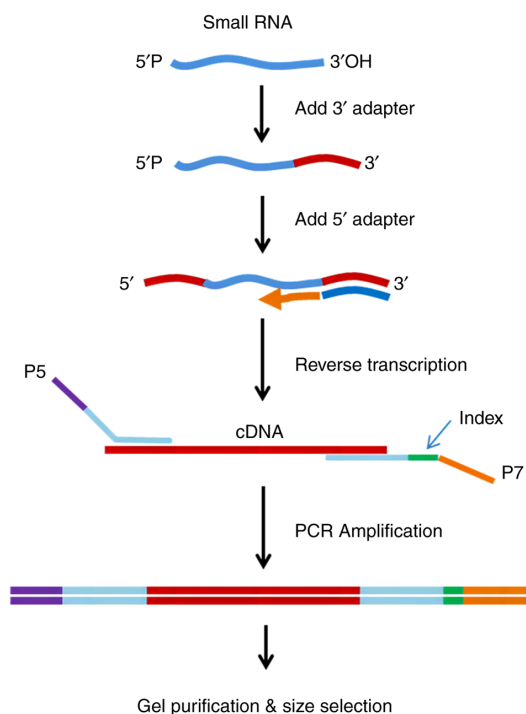

Figure 1. Schematic of library construction. Using the special structure of the 3' and 5' ends of small RNA (the 5' end has a complete phosphate group and the 3' end has a hydroxyl group) and total RNA as the starting sample, the two ends of the small RNA were directly added to the adapter and then the cDNA was synthesized by reverse transcription. After PCR amplification, the target DNA fragment was separated by SDS-PAGE and the cDNA library was recovered.

Differential expression analysis of known miRNAs. The input data of miRNA differential expression were readcount data obtained from the miRNA analysis. The samples of the present study were biological duplicates. For samples with biological replicates, differential expression analysis of two groups was performed using DESeq 1.2.10 (http://www.bioconductor.org/packages/release/bioc/html/DESeq2.html). The cutoff critera for differential expression were as follows: $P_{adjusted}<0.001$ and |log2 fold-change (FC)| >2.5. The miRNAs screened in the aforementioned steps were differentially expressed miRNAs, which were subjected to downstream analysis.

Functional analysis of significantly differentially expressed miRNAs. The target genes of miRNAs were predicted using miRanda (13) and RNAhybrid (14). The hairpin structure of miRNA precursors was used to predict novel miRNAs. The software miREvo (15) and mirdeep2 (16) were integrated to predict novel miRNAs by exploring the secondary structure. The dicer cleavage site and minimum free energy of the small RNA tags were unannotated in the previous steps. In addition, custom scripts were used to obtain the identified miRNA counts as well as base bias at the first position with a certain length and at each position of all the identified miRNAs. Upon obtaining the significantly differentially expressed miRNAs in the GLM and control groups. according to the significantly differentially expressed miRNAs and their target genes, Gene Ontology (GO; http://www.geneontology.org/) and Kyoto Encyclopedia of Genes and Genomes (KEGG; https://www.kegg.jp/) enrichment were performed in the two groups of target genes. The GO sequencing-based Wallenius' noncentral hypergeometric distribution, which was able to adjust for gene length bias, was then implemented for GO enrichment analysis. KOBAS software (17) (v2.0; cut-off, blastx 1x10^{-5}; P_{adjust}: Benjamini-Hochberg) was used to assess the statistical enrichment of the target gene candidates in the KEGG pathways.

Validation of differentially expressed miRNAs by reverse transcription-quantitative (RT-q)PCR. In total, 24 serum samples were used for RT-qPCR, which was performed to

confirm the sequencing data. The donors were patients that were not included in the other analyses but recruited during the same period. The demographic and clinicopathological characteristics of the two groups are recorded in Table SI. A total of 12 upregulated miRNAs [miR-451a, miR-5571-3p, miR-106a-5p, miR-20b-5p, miR-223-5p, miR-3916, miR-4433a-3p, miR-4433b-5p, miR-4659a-3p, miR-4802-3p, miR-624-5p and miR-942-3p] were selected for RT-qPCR. The Serum RNA Extraction Kit (Beijing ComWin Biotech Co., Ltd.) was used to isolate total RNA from breast tissue samples. The concentration of total RNA was determined by UV spectrophotometry. Next, the absorbance value was measured at 260 and 280 nm with a BIO-DL micro Drop (Shanghai Woyuan Technology Co., Ltd.) and the concentration and purity were calculated. According to the manufacturer's instructions, an miRNA RT Kit (Comwin Biotech Co., Ltd.) was used for cDNA synthesis, to reverse-transcribe RNA into cDNA. Next, the cDNA was used to perform real-time qPCR. The internal control for normalization was H-U6. The primers designed for the amplification of the miRNA transcripts are listed in Table II.

RT-qPCR was performed in a 30-μl reaction volume. Triplicate wells were set for all samples and references. The results were calculated by the $2^{-\Delta\Delta Cq}$ method (18) and displayed as the mean ± standard deviation. Graphical presentation of the results was performed using GraphPad Prism 8 (GraphPad Software, Inc.). The reaction components were as follows: Template (cDNA), 2 μl; 10 μM forward primer, 1 μl; 10 μM reverse primer, 1 μl; double-distilled H$_2$O, 11 μl; and 2X SYBR Green PCR Master Mix (Beijing ComWin Biotech Co., Ltd.), 15 μl. The reaction was performed in the fluorescence quantitative RCP instrument QuantStudio1 (Applied Biosystems, Inc.). The thermocycling conditions were as follows: 95℃ for 10 min, followed by 95℃ for 15 sec and 60℃ for 30 sec (15-30 cycles for most products; 31-33 cycles for certain other products). PCR melting curve analysis was performed at 60-95℃.

Statistical analysis. Values are expressed as the mean ± standard deviation. Statistical analyses were performed using SPSS 21.0 (IBM Corporation). If the two sets of data conformed to a normal distribution, a 2-independent-samples t-test was used for analysis; otherwise, a 2-independent-samples Mann-Whitney U-test was used for analysis. P<0.05 was considered to indicate a statistically significant difference.

Results

Basic content analysis of small RNA library. Total reads were obtained from high-throughput sequencing of the GLM and control groups. Next, clean reads with a high base quality were screened from the total reads. Clean reads were used for miRNA detection and new miRNA prediction (Fig. 2). Differential miRNAs, upregulated miRNAs and downregulated miRNAs were obtained by comparing the GLM and control groups (Table III). The TPM density distribution was determined to evaluate the gene expression pattern of the samples as a whole (Fig. 3). Overall, the TPM density distribution was concentrated in the interval 0-2 and the TPM density distribution of the control group was closer to 0 than that of the GLM group.

Table II. Sequences of PCR primers.

miRNA name	Sequence (5'-3')
miR-106a-5p	AAAAGTGCTTACAGTGCAGGTAG
miR-20b-5p	CAAAGTGCTCATAGTGCAGGTAG
miR-223-5p	CGTGTATTTGACAAGCTGAGTT
miR-3916	AAGAGGAAGAAATGGCTGGTTCTCAG
miR-4433a-3p	ACAGGAGTGGGGGTGGGACAT
miR-4433b-5p	ATGTCCCACCCCCACTCCTGT
miR-451a	AAACCGTTACCATTACTGAGTT
miR-4659a-3p	TTTCTTCTTAGACATGGCAACG
miR-4802-3p	TACATGGATGGAAACCTTCAAGC
miR-5571-3p	GTCCTAGGAGGCTCCTCTG
miR-624-5p	TAGTACCAGTACCTTGTGTTCA
miR-942-3p	CACATGGCCGAAACAGAGAAGT
H-U6	
Forward	CTCGCTTCGGCAGCACA
Reverse	AACGCTTCACGAATTTGCGT

For the miRNAs, a universal reverse primer included in the kit was used. miR/miRNA, microRNA.
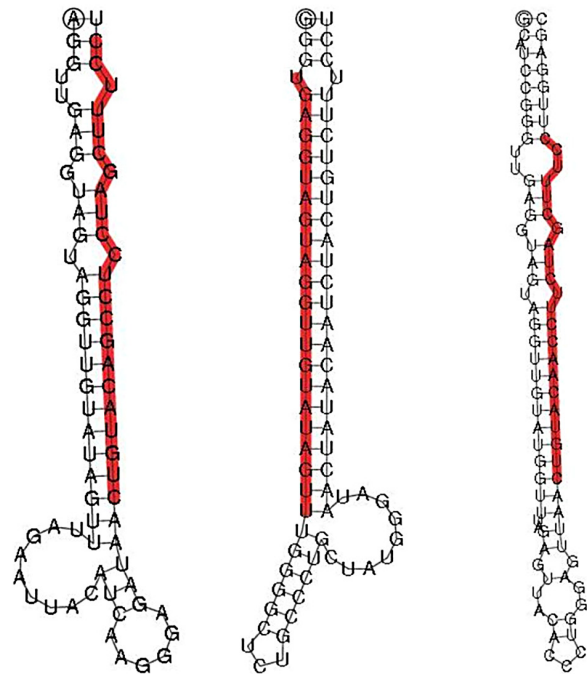

Figure 2. Secondary structure of certain known miRNAs. The canonical hairpin structure of miRNAs may be used to predict novel miRNAs. The entire sequence is miRNA precursor and the red part is the mature sequence. The three novel predicted secondary structures in the figure differ in the number of internal loops, the number of hairpin loops and the length of the stems. miRNA, microRNA.

The correlation of gene expression levels between samples (Fig. 4) was an important index to assess the reliability of the experiments and the rationality of the sample selection. A correlation coefficient R2 closer to 1 indicated a higher similarity of expression patterns between samples.

Table III. Basic content of the small RNA library.

Item	GLM	Control
Total reads	14,24,89,416	14,85,52,630
Clean reads	12,48,65,556	13,01,44,449
Mature miRNA	9,603	6,536
Hairpin miRNA	8,361	5,712
Novel mature miRNA	267	138
Novel hairpin miRNA	311	149
Differential miRNAs[a]	186	Ref.
Upregulated miRNAs	127	Ref.
Downregulated miRNAs	59	Ref.

[a]Comparison with control group. miRNA, microRNA; GLM, granulomatous lobular mastitis.
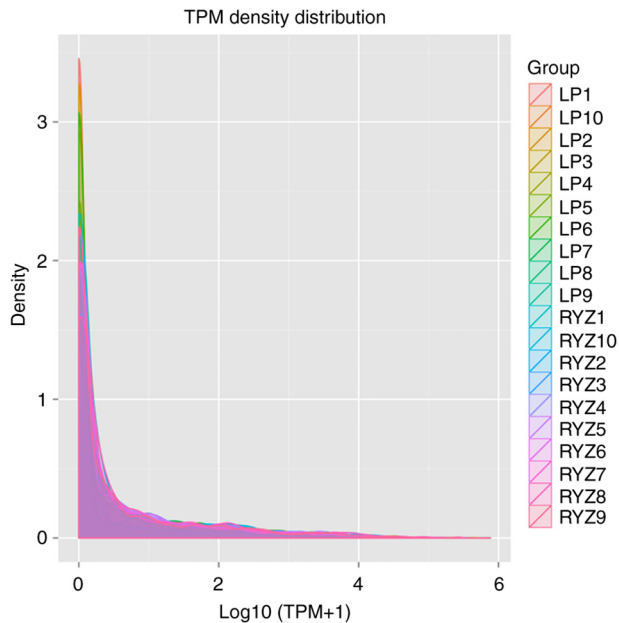
Figure 3. TPM density distribution. LP1-10 are the control samples (n=10) and RYZ1-10 are the granulomatous lobular mastitis samples (n=10). The X-axis indicates the log10 (TPM+1) value of microRNAs and the Y-axis the density of the log10 (TPM+1).

Differential miRNAs in tissue in the GLM and control groups. Under the condition of the significance threshold |log2FC|>2.5 and q<0.001, The volcano plot of differential miRNAs revealed that 7 downregulated miRNAs in the GLM vs. control group (represented with green dots) exhibited significant differences in expression, including hsa-miR-129-5p, hsa-miR-135a-2-3p, hsa-miR-211-5p, hsa-miR-375-3p, hsa-miR-483-3p, hsa-miR-488-5p and hsa-miR-6507-5p; and 39 upregulated miRNAs (represented with red dots) in the GLM vs. control group were significantly differentially expressed, including hsa-miR-106a-5p, hsa-miR-1255b-5p, hsa-miR-1273c, hsa-miR-130b-3p, hsa-miR-142-3p, hsa-miR-142-5p, hsa-miR-146a-5p, hsa-miR-1537-3p, hsa-miR-155-5p, hsa-miR-20b-5p, hsa-miR-223-5p, hsa-miR-3614-3p, hsa-miR-3916, hsa-miR-4433a-3p, hsa-miR-4433b-5p,

hsa-miR-451a, hsa-miR-4659a-3p, hsa-miR-4659b-5p, hsa-miR-4772-3p, hsa-miR-4802-3p, hsa-miR-518a-3p, hsa-miR-518c-5p, hsa-miR-518f-3p, hsa-miR-5193, hsa-miR-519c-5p, hsa-miR-519d-3p, hsa-miR-522-3p, hsa-miR-524-5p, hsa-miR-525-5p, hsa-miR-548d-3p, hsa-miR-548j-5p, hsa-miR-549a-3p, hsa-miR-549a-5p, hsa-miR-5571-3p, hsa-miR-624-5p, hsa-miR-643, hsa-miR-660-3p, hsa-miR-942-3p and hsa-miR-942-5p. There were more upregulated than downregulated miRNAs (Fig. 5). Based on this, the differentially expressed miRNAs of 10 samples in the GLM group that were all higher/lower than those in the control group may be screened by clustering analysis.

Using the threshold of |log2FC|>2.5 and q<0.001, clustering analysis of differentially expressed miRNAs revealed 13 miRNAs with higher expression in the GLM group than in the control group, including hsa-miR-106a-5p (|log2FC|=3.0698), hsa-miR-155-5p (|log2FC|=3.4676), hsa-miR-20b-5p (|log2FC|=3.4475), hsa-miR-223-5p (|log2FC|=3.2646), hsa-miR-3916 (|log2FC|=3.1171), hsa-miR-4433a-3p (|log2FC|=3.3266), hsa-miR-4433b-5p (|log2FC|=3.3266), hsa-miR-451a (|log2FC|=3.1156), hsa-miR-4659a-3p (|log2FC|=3.2052), hsa-miR-4802-3p (|log2FC|=3.218), hsa-miR-5571-3p (|log2FC|=3.4794), hsa-miR-624-5p (|log2FC|=2.6682) and hsa-miR-942-3p (|log2FC|=3.2555). However, no miRNAs were observed to exhibit lower expression in the GLM group than in the control group (Fig. 6).

Enrichment analysis of differentially expressed miRNA target genes. GO (http://www.geneontology.org/) is the international standard classification system for gene function. In the present study, GO analysis was performed according to the results of 13 differentially expressed miRNAs. Studying the distribution of candidate target genes by GO clarified the expression differences among the samples according to gene function. Among them, GO:0009987 cellular process biological_process (18301), GO:0005623 cell cellular_component (19013), GO:0044464 cell part cellular_component (18940) and GO:0005488 binding molecular_function (17470) were the most significantly enriched GO terms (Fig. 7).

In living organisms, different genes coordinate biological functions. Pathway significant enrichment may identify the main biochemical metabolic pathways and signal transduction pathways involving candidate target genes. KEGG is a major public database of signaling pathways (19). The degree of enrichment in KEGG was determined by the rich factor, q-value and number of genes enriched in pathways. The corrected q-value was 0.999804687. The top 10 enriched KEGG pathways were folate biosynthesis, sulfur relay system, vitamin digestion and absorption, glycosaminoglycan biosynthesis-keratan sulfate, pyruvate metabolism, dilated cardiomyopathy, axon guidance, chagas disease (American trypanosomiasis), hypertrophic cardiomyopathy and measles. Among them, folate biosynthesis (rich factor, 0.5), sulfur relay system (rich factor, 0.4) and vitamin digestion and absorption (rich factor, 0.375) were the most significantly enriched KEGG pathways (Fig. 8).

Target genes of differentially expressed miRNAs. A total of 3,072 target RNAs of the aforementioned 13 miRNAs were determined. There were 349 co-regulated target genes
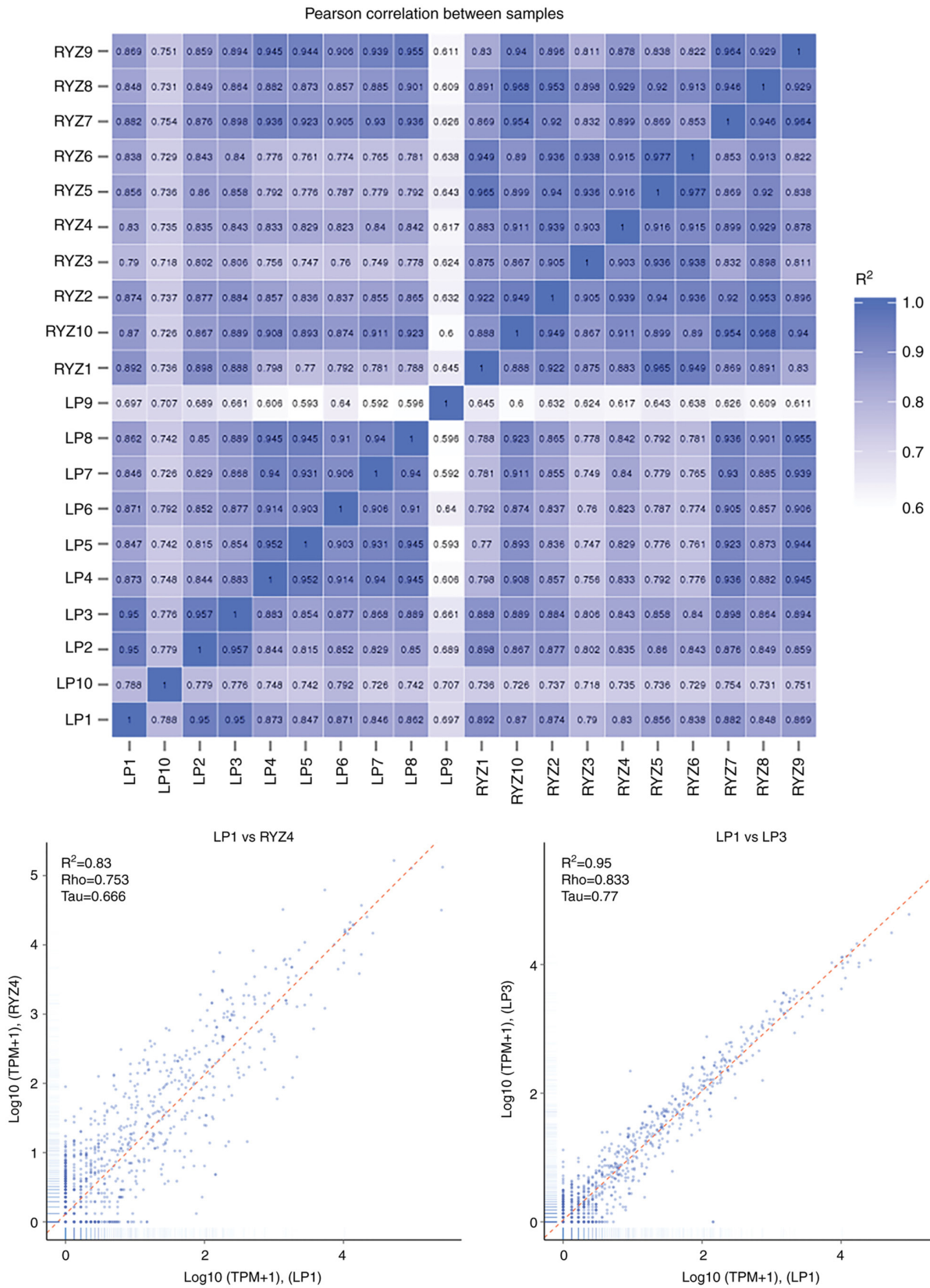
Figure 4. Correlation of gene expression levels between samples. LP1-10 are the control group (n=10) and RYZ1-10 are the granulomatous lobular mastitis group samples (n=10). In the correlation plots, the abscissa and ordinate present the log10 (TPM+1) for each miRNA. R2, square of Pearson's correlation coefficient; Rho, Spearman correlation coefficient; Tau, Kendall-tau correlation coefficient.

between miRNAs. miR-106a-5p regulated 158 target genes; miR-155-5p regulated 5 target genes; miR-20b-5p regulated 252 target genes; miR-223-5p regulated 5 target genes; miR-3916 regulated 366 target genes; miR-4433a-3p regulated 1,242 target genes; miR-4433b-5p regulated 626 target genes; miR-4659a-3p regulated 20 target genes; miR-4802-3p
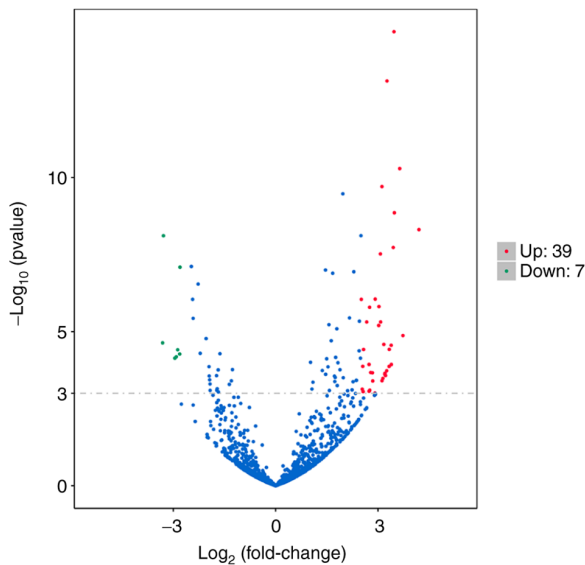
Figure 5. Volcano plot of differential miRNAs in the GLM and control groups. The Y-axis presents the-log10 (P-value) for each miRNA and indicates the significance level of differential miRNAs. The X-axis presents the |log2FC| and indicates the FC of miRNA expression in the GLM and control groups. A larger |log2FC| indicates a larger difference in expression between the two groups. Green dots represent downregulated miRNAs, red dots represent upregulated miRNAs and blue dots indicate miRNA with insignificant changes. GLM, granulomatous lobular mastitis; miRNA, microRNA; FC, fold change.
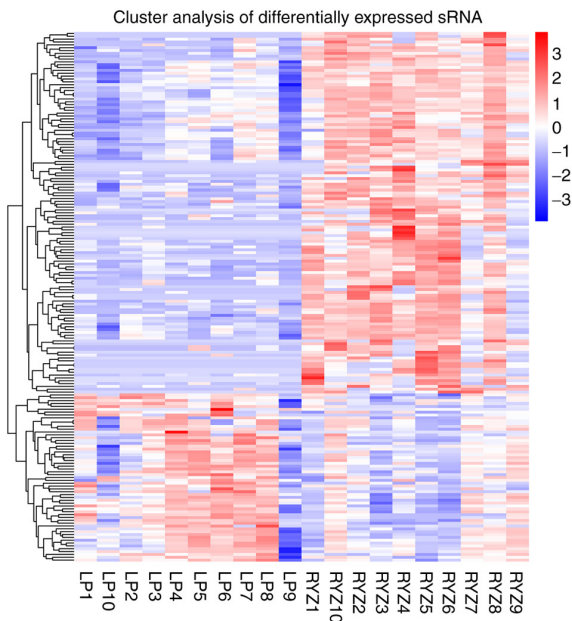

Figure 6. Cluster analysis of differential miRNAs in the GLM and control groups. Log10 (TPM+1) values are used for clustering, red represents upregulated miRNAs and blue represents downregulated miRNAs. A darker color indicates a more significant upregulation or downregulation. The X-axis represents the different samples in the cluster analysis. LP1-10 are the control group (n=10) and RYZ1-10 are the GLM group (n=10). The Y-axis represents the differential microRNAs. GLM, granulomatous lobular mastitis; sRNA, small RNA.

regulated 22 target genes; miR-5571-3p regulated 311 target genes; miR-624-5p regulated 27 target genes; and miR-942-3p regulated 38 target genes. The co-regulated target genes

included RAPGEFL1, FOSB, CFLAR, CAMKK1, MAP3K9, STX10 and PBLD.

Validation of differentially expressed miRNAs. Based on the present sequencing results and previous studies published in the literature, the plasma levels of 12 differentially expressed miRNAs were further analyzed in two groups of 12 patients with GLM and 12 controls by RT-qPCR. As presented in Fig. 9, a statistically significant increase in miR-451a and miR-5571-3p expression was observed, which was consistent with the sequencing results. However, the present study failed to validate the RNA sequencing results in terms of the increased levels of miR-106a-5p, miR-20b-5p, miR-223-5p, miR-3916, miR-4433a-3p, miR-4433b-5p, miR-4659a-3p, hsa-miR-4802-3p, miR-624-5p and miR-942-3p in GLM. The level of miR-20b was undetectable in almost all samples (both GLM and controls).

Discussion

The etiology and pathogenesis of GLM are still poorly understood. Current surgical procedures and medical treatments for GLM are frequently accompanied by numerous complications and a high recurrence rate (20,21). In recent years, technologies such as noninvasive biomarkers and miRNA chips have emerged, which may contribute to the diagnosis of diseases. These latest techniques may evolve until becoming the novel gold standard diagnostic tool, thereby eliminating invasive biopsy.

The demographic characteristics and laboratory findings of the GLM and control groups were statistically analyzed in the present study, and it was observed that the number of white blood cells was significantly increased in the GLM group. There were no obvious abnormalities in other biochemical indexes, which directly supported the notion that GLM is an inflammatory disease. Sequencing was used for GLM tissues and for normal tissues located next to the fibroadenoma, and 186 different miRNAs were identified, among which 127 genes were upregulated and 59 genes were downregulated in the GLM group.

Differentially expressed miRNAs in patients with GLM were screened by setting the threshold |log2FC|>2.5 and q<0.001. These miRNAs have rarely been reported in previous studies on GLM, but have been mentioned in upstream pathways or as biomarkers for immune and cancer diseases in various studies. Aksan *et al* (12) reported that the serum levels of miR-155 and let-7c were significantly reduced in patients with BC and GLM, but they were not able to be used as biomarkers to distinguish GLM and BC, as there was no significant difference between them. Therefore, miR-155-5p may be excluded in subsequent clinical validation studies. GO and KEGG enrichment analysis suggested that the occurrence and development of GLM may be associated with autoimmune inflammation, metabolism and pathogenic organisms.

The association between GLM and inflammation is markedly high. The hypothesis that GLM is an autoimmune inflammatory disease has been supported by epidemiology, clinical manifestations and the effects of immunosuppressive therapy, as well as serological and histopathological evidence. Koksal (22) retrospectively analyzed 134 patients diagnosed
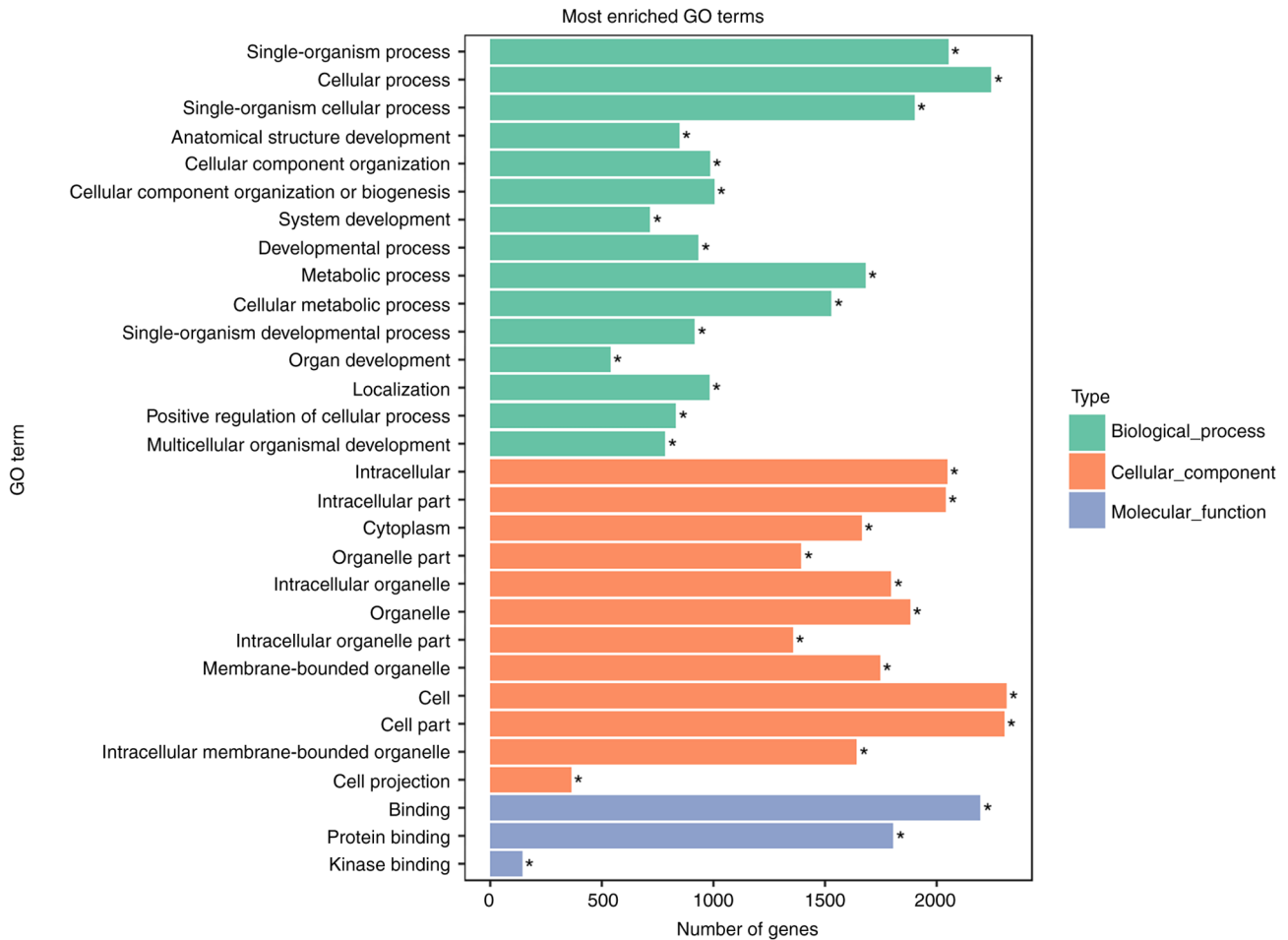
Figure 7. The most significantly enriched GO terms. The X-axis presents the number of candidate target genes annotated to the term and their proportion to the total number of candidate target genes. Asterisks on the bar charts represent significant enrichment of the respective pathway. GO, Gene Ontology.

with GLM. Seasonal fluctuations were noticed, with the incidence being slightly higher during late spring and summer. Seasonal fluctuations suggested the possibility of an immunological disease rather than a resectable disease requiring surgical treatment. In addition, patients may have clinical manifestations of systemic inflammatory responses during the course of GLM, such as polyangiitis (23), erythema nodosum, fever and arthritis (24). Drugs for the treatment of GLM are currently under investigation. Although no consensus has been reached on the selection of drugs, corticosteroids (20,25,26) and methotrexate (27,28) have been widely used in the treatment of GLM. GLM is considered to be an autoimmune inflammatory disease due to the marked clinical treatment effect of immunosuppressants. Chiu *et al* (29) reported that the breast symptoms of patients with GLM resolved following treatment with the tumor necrosis factor (TNF)-α inhibitor adalimumab. TNF-α is involved in systemic inflammation and is one of the cytokines that stimulate the acute-phase response. Inflammation-related factors, including IL-17, IL-22 and IL-23, were reported to be significantly increased in GLM (30), and autoantibodies such as rheumatoid factor, antinuclear antibody and anti-double-stranded DNA were positive (31). Huang *et al* (32) indicated that serum IL-6 and C-reactive protein levels may be used as biomarkers to evaluate the severity and prognosis of GLM. Histopathologically, GLM was characterized by a

significant granulomatous inflammatory reaction centered on lobules, with granuloma and microabscess formation within the lobules and surrounding tissue, and with multinucleated giant cell infiltration. Neutrophils were the most common type of lobular inflammatory cells, followed by lymphocytes (33).

α-1-Antitrypsin deficiency (AATD) and smoking as a metabolic factor may be associated with the onset of GLM. Local heat therapy may be used to treat GLM, which may explain the association between GLM and metabolism. Schelfout *et al* (34) reported on a 37-year-old woman with AATD associated with GLM. Physiologically, AAT is the major inhibitor of elastase produced by neutrophils and has a wide range of anti-proteolytic and anti-inflammatory actions. It functions as an acute-phase reactant, increasing its levels to respond to inflammatory or infectious phenomena. AATD causes inflammation due to an inadequate anti-inflammatory capacity. The Z allele is referred to a point mutation causing an amino acid change from glutamic acid to lysine at position 342 (Glu342Lys), in which the AAT plasma levels are <35% of the mean expected value. The acute stage of GLM is frequently accompanied by local breast skin redness, swelling, heat and pain, with certain patients experiencing recurrent fever. Increased temperature, elevated Z-AAT concentration and acidosis, all of which may occur at the sites of tissue inflammation *in vivo*, were observed to enhance AAT polymerization *in vitro*. It was hypothesized
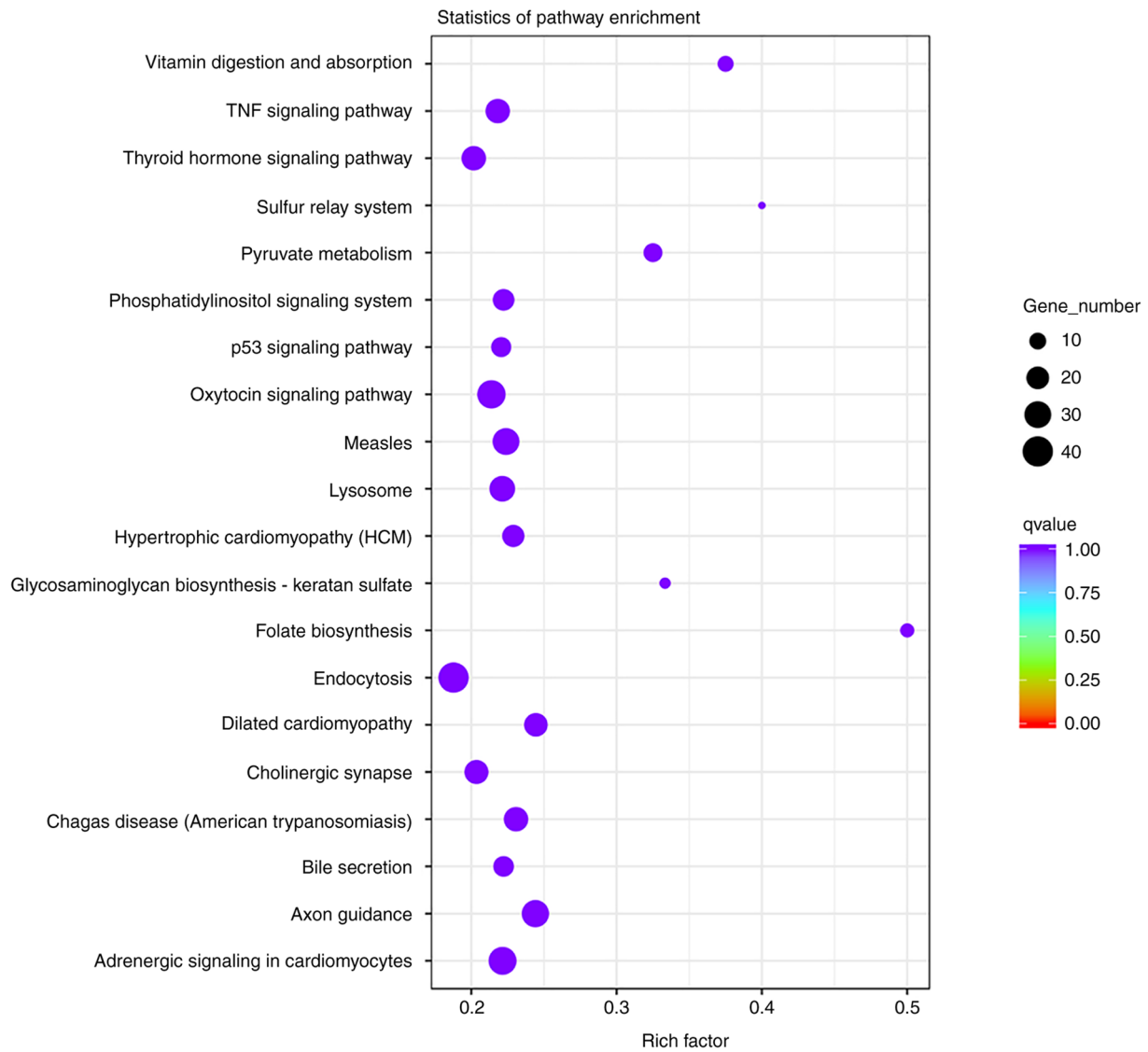
Figure 8. The most significantly enriched Kyoto Encyclopedia of Genes and Genomes pathways. The dot size indicates the number of candidate target genes in this pathway. The colour of the dots corresponds to different q-value ranges. The Rich factor refers to the ratio of the number of differentially expressed genes located in this pathway and the number of genes located in this pathway among all annotated genes. The larger the Rich factor, the greater the degree of enrichment. The range of the q-value is 0-1.

that the increased secretion of AAT compensated the insufficient anti-inflammatory ability caused by the absence of ATT in long-term local inflammatory responses, which may also explain the self-limiting nature of GLM that has been reported by several studies (35,36). Li *et al* (35) retrospectively analyzed 15 cases of pregnancy-associated granulomatous mastitis. Almost all patients were selected for observation during pregnancy. In total, 9 patients experienced complete remission. Çetinkaya *et al* (36) retrospectively evaluated 118 female patients diagnosed with IGM; of them, 42.4% recovered under observation without any treatment and the mean recovery period was 5.6 months. Accumulation of Z-AAT polymers within the endoplasmic reticulum of neutrophils leads to endoplasmic reticulum stress, increased neutrophil apoptosis and defective bacterial killing (37). This may also explain the insensitivity of GLM to antibiotics, which were used in 33/36 (91.7%) patients in a previous study by Williams *et al* (38). The mean duration of antibiotic therapy was 7.0±4.5 months.

Although no studies have directly compared antibiotics with the 'watch and wait' approach, the antibiotics in the above study were used for a markedly longer time than the usual course of treatment. At present, there is only a small number of studies on ATT in GLM. To better understand the function of AAT in GLM and the role of AAT augmentation therapy (α1-proteinase inhibitor) in deficiency states, further experiments are required to verify the effectiveness of AAT augmentation therapy in processing GLM.

Previous studies have demonstrated that GLM is associated with smoking. A 10-year study from a multi-center clinical database in China indicated that smoking and *Corynebacterium* infection are risk factors for recurrence of GLM (39). A multicenter study involving 720 patients with GLM determined a correlation between smoking and GLM (40). Tang *et al* (41) indicated that smokers had a 10-fold probability of exhibiting IGM compared to patients who did not smoke. Although there is no direct evidence
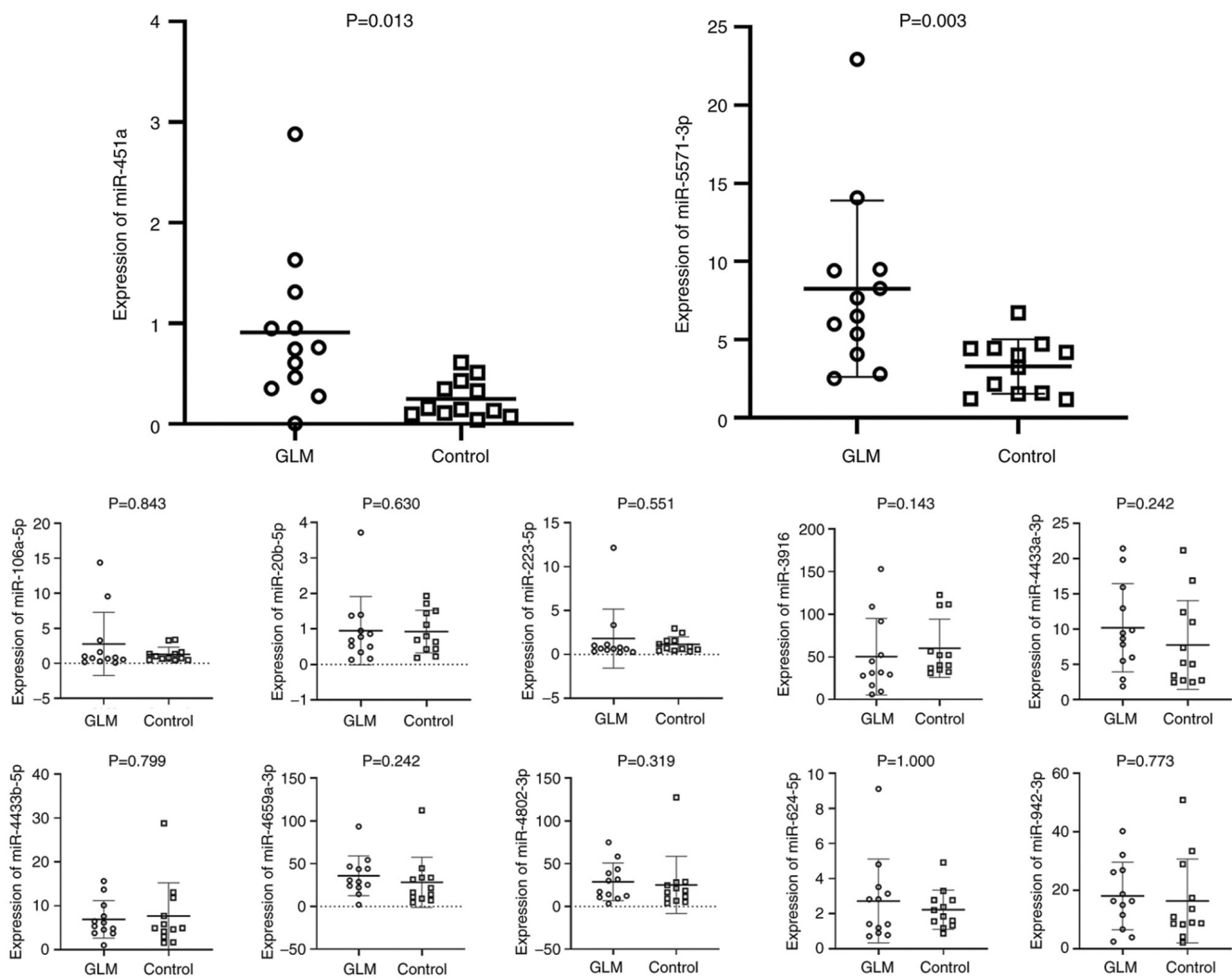
Figure 9. Validation of 12 differentially expressed miRNAs between the two groups using reverse transcription-quantitative PCR. The Y-axis represents the differential miRNA expression. miRNA, microRNA; GLM, granulomatous lobular mastitis.

to demonstrate that metabolite abnormalities caused by smoking may induce GLM, indirect studies suggested that smoking may cause a variety of metabolic abnormalities in the body. Hu *et al* (42) reported that smoking is associated with variations in the concentration of sphingolipids and glycerophospholipids, and in amino acid metabolism. Among non-single, young and generally healthy city dwellers, cigarette smokers had a 2.4-fold greater risk of developing metabolic syndrome compared with that of non-cigarette smokers, and the risk of developing hypertriglyceridemia and low high-density lipoprotein cholesterolemia was also higher (43).

Chen *et al* (44) indicated that local heat therapy was able to treat GLM. The optimum growth temperature for *Corynebacterium kroppenstedtii* (*C. kroppenstedtii*) was 37˚C and its growth was inhibited at 42˚C; thus, local temperature control may result in growth arrest of *C. kroppenstedtii*. However, the efficacy of antibiotics in treating GLM is limited. When the ambient temperature is >30˚C, the reaction speed of chemical processes in the body is accelerated and energy metabolism is also enhanced. Whether the curative effect achieved through hyperthermia for GLM is associated with

the enhancement of local metabolism should be investigated in future experiments.

Previous studies demonstrated a correlation between GLM and pathogenic organisms. Although pathogenic organisms responsible for GM have not been fully identified, numerous studies detected the possible presence of pathogenic organisms through bacterial culture and sequencing methods (45-47). Among them, *C. kroppenstedtii* was reported more frequently. Gram-positive bacilli, non-tuberculosis mycobacteria, *C. kroppenstedtii* and *Pseudomonas oleovorans*, *C. kroppenstedtii* and human g herpes virus, *Acinetobacter baumannii* and *C. kroppenstedtii*, *Rickettsia*, mixed infection of various bacteria and other bacteria, have also been reported. The use of various detection methods to identify specific pathogenic organisms and select sensitive antibiotics is an important way to treat GLM.

In the present study, the expression of miR-451a and miR-5571-3p was verified to be higher in the GLM group than in the normal group. miR-451a has not only been indicated to be involved in various immune inflammatory diseases such as systemic lupus erythematosus (10) and experimental allergic encephalomyelitis (11), but has also been implicated in the initiation and progression of BC. Zhang *et al* (48) indicated that

overexpression of miR-451a repressed BC cell proliferation, migration and invasion. Therefore, whether miR-451a may become a biomarker for GLM requires to be further evaluated. In a similar study, analyses of miRNA profile sequencing revealed that miR-5571-3p correlates with an increased disease risk and activity of rheumatoid arthritis (49). miR-451-a and miR-5571-3p are associated with inflammatory diseases and may regulate the pathogenesis of GLM.

In summary, the present study investigated the differentially expressed miRNAs associated with GLM and normal tissues, and their differential expression was verified by using clinical specimens. However, the present study had several limitations, including a small sample size and the fact that the mechanisms by which the identified differentially expressed miRNAs influence GLM were not investigated. Thus, in future studies, the sample size should be increased for further validation of the GLM-associated differentially expressed miRNAs, and the mechanisms underlying the action of different genes should be investigated in animal models.

Availability of data and materials

The datasets used and/or analyzed during the current study are available from the corresponding author on reasonable request.

Authors' contributions

HF and LL conceived and designed the current study. WH, JLu and YW collected clinical data and specimens. JLi and XX analyzed data. JS and SW performed the RT-qPCR validation experiments. JS and SW checked and approved the authenticity of the raw data. All authors read and approved the final manuscript.

Ethics approval and consent to participate

The study was approved by the Ethics Committee of the First Hospital of Hunan University Of Chinese Medicine (Changsha, China; April 2019; no. HN-LL-ZFKY-2019-004-01) and was conducted in accordance with the Declaration of Helsinki. Written informed consent was obtained from all volunteers. The informed consent was provided in triplicate, including one for the patient, one for the investigator and one for the Biological Specimen Banks.

Patient consent for publication

Not applicable.

Competing interests

The authors declare that they have no competing interests.

References

1. Li J: Diagnosis and treatment of 75 patients with idiopathic lobular granulomatous mastitis. J Invest Surg 32: 414-420, 2019.
2. Parperis K, Achilleos S, Costi E and Vardas M: Granulomatous mastitis, erythema nodosum and arthritis syndrome: Case-based review. Rheumatol Int 41: 1175-1181, 2021.
3. Toprak N, Toktas O, Ince S, Gunduz AM, Yokus A, Akdeniz H and Ozkacmaz S: Does ARFI elastography complement B-mode ultrasonography in the radiological diagnosis of idiopathic granulomatous mastitis and invasive ductal carcinoma. Acta Radiol 63: 28-34, 2020.
4. Emsen A, Köksal H, Özdemir H, Kadoglou N and Artaç H: The alteration of lymphocyte subsets in idiopathic granulomatous mastitis. Turk J Med Sci 51: 1905-1911, 2021.
5. Ucaryilmaz H, Koksal H, Emsen A, Kadoglou N, Dixon JM and Artac H: The role of regulatory T and B cells in the etiopathogenesis of idiopathic granulomatous mastitis. Immunol Invest 51: 357-367, 2022.
6. Li XQ, Yuan JP, Fu AS, Wu HL, Liu R, Liu TG, Sun SR and Chen C: New insights of *Corynebacterium kroppenstedtii* in granulomatous lobular mastitis based on nanopore sequencing. J Invest Surg 35: 639-646, 2022.
7. Naik MA, Korlimarla A, Shetty ST, Fernandes AM and Pai SA: Cystic neutrophilic granulomatous mastitis: A clinicopathological study with 16s rRNA sequencing for the detection of corynebacteria in formalin-fixed paraffin-embedded tissue. Int J Surg Pathol 28: 371-381, 2020.
8. Huang Y and Wu H: A retrospective analysis of recurrence risk factors for granulomatous lobular mastitis in 130 patients: More attention should be paied to prolactin level. Ann Palliat Med 10: 2824-2831, 2021.
9. O'Brien J, Hayder H, Zayed Y and Peng C: Overview of MicroRNA biogenesis, mechanisms of actions, and circulation. Front Endocrinol (Lausanne) 9: 402, 2018.
10. Shi G, Li D, Zhang D, Xu Y, Pan Y, Lu L, Li J, Xia X, Dou H and Hou Y: IRF-8/miR-451a regulates M-MDSC differentiation via the AMPK/mTOR signal pathway during lupus development. Cell Death Discov 7: 179, 2021.
11. Nakashima M, Ishikawa K, Fugiwara A, Shu K, Fukushima Y, Okamoto M, Tsukamoto H, Kouwaki T and Oshiumi H: miR-451a levels rather than human papillomavirus vaccine administration is associated with the severity of murine experimental autoimmune encephalomyelitis. Sci Rep 11: 9369, 2021.
12. Aksan H, Kundaktepe BP, Sayili U, Velidedeoglu M, Simsek G, Koksal S, Gelisgen R, Yaylim I and Uzun H: Circulating miR-155, let-7c, miR-21, and PTEN levels in differential diagnosis and prognosis of idiopathic granulomatous mastitis and breast cancer. Biofactors 46: 955-962, 2020.
13. Enright AJ, John B, Gaul U, Tuschl T, Sander C and Marks DS: MicroRNA targets in Drosophila. Genome Biol 5: R1, 2003.
14. Krüger J and Rehmsmeier M: RNAhybrid: microRNA target prediction easy, fast and flexible. Nucleic Acids Res 34 (Web Server Issue): W451-W454, 2006.
15. Wen M, Shen Y, Shi S and Tang T: miREvo: An integrative microRNA evolutionary analysis platform for next-generation sequencing experiments. BMC Bioinformatics 13: 140, 2012.
16. Friedländer MR, Mackowiak SD, Li N, Chen W and Rajewsky N: miRDeep2 accurately identifies known and hundreds of novel microRNA genes in seven animal clades. Nucleic Acids Res 40: 37-52, 2012.
17. Mao X, Cai T, Olyarchuk JG and Wei L: Automated genome annotation and pathway identification using the KEGG Orthology (KO) as a controlled vocabulary. Bioinformatics 21: 3787-3793, 2005.
18. Schmittgen TD and Livak KJ: Analyzing real-time PCR data by the comparative C(T) method. Nat Protoc 3: 1101-1108, 2008.
19. Kanehisa M, Araki M, Goto S, Hattori M, Hirakawa M, Itoh M, Katayama T, Kawashima S, Okuda S, Tokimatsu T and Yamanishi Y: KEGG for linking genomes to life and the environment. Nucleic Acids Res 36 (Database Issue): D480-D484, 2008.
20. Ertürk TF, Çakır Ö, Yaprak Bayrak B, Güneş A, Aydemir S and Utkan NZ: Local steroid treatment: An effective procedure for idiopathic granulomatous mastitis, including complicated cases. J Invest Surg 35: 745-751, 2022.

21. Ringsted S and Friedman M: A rheumatologic approach to granulomatous mastitis: A case series and review of the literature. Int J Rheum Dis 24: 526-532, 2021.
22. Koksal H: What are the new findings with regard to the mysterious disease idiopathic granulomatous mastitis? Surg Today 51: 1158-1168, 2021.
23. Ip KH, Koch K and Lamont D: Granulomatosis with polyangiitis: A life-threatening cause of granulomatous mastitis. ANZ J Surg 91: E59-E60, 2021.
24. Luo W, Xu B, Wang L, Xiang L, Lai M, Zhang X and Liu X: Clinical characteristics and predictive factors of erythema nodosum in granulomatous lobular mastitis. Australas J Dermatol 62: 342-346, 2021.
25. Yildirim E, Kayadibi Y, Bektas S, Ucar N, Oymak A, Er AM, Senturk A and Demir IA: Comparison of the efficiency of systemic therapy and intralesional steroid administration in the treatment of idiopathic granulomatous mastitis. The novel treatment for granulomatous mastitis. Ann Ital Chir 92: 234-241, 2021.
26. Toktas O, Konca C, Trabulus DC, Soyder A, Koksal H, Karanlik H, Kamali Polat A, Ozbas S, Yormaz S, Isik A, *et al*: A novel first-line treatment alternative for noncomplicated idiopathic granulomatous mastitis: Combined intralesional steroid injection with topical steroid administration. Breast Care (Basel) 16: 181-187, 2021.
27. Postolova A, Troxell ML, Wapnir IL and Genovese MC: Methotrexate in the treatment of idiopathic granulomatous mastitis. J Rheumatol 47: 924-927, 2020.
28. Kafadar MT, Bahadır MV and Girgin S: Low-dose methotrexate use in idiopathic granulomatous mastitis: An alternative treatment method. Breast Care (Basel) 16: 402-407, 2021.
29. Chiu LW, Goodwin K, Vohra P and Amerson E: Cystic neutrophilic granulomatous mastitis regression with the tumor necrosis factor-α inhibitor, adalimumab. Eur J Breast Health 18: 94-101, 2021.
30. Saydam M, Yilmaz KB, Sahin M, Yanik H, Akinci M, Yilmaz I, Balas S, Azili C and Gulcelik MA: New findings on autoimmune etiology of idiopathic granulomatous mastitis: Serum IL-17, IL-22 and IL-23 levels of patients. J Invest Surg 34: 993-997, 2021.
31. Ozel L, Unal A, Unal E, Kara M, Erdoğdu E, Krand O, Güneş P, Karagül H, Demiral S and Titiz MI: Granulomatous mastitis: Is it an autoimmune disease? Diagnostic and therapeutic dilemmas. Surg Today 42: 729-733, 2012.
32. Huang YM, Lo C, Cheng CF, Lu CH, Hsieh SC and Li KJ: Serum C-reactive protein and interleukin-6 levels as biomarkers for disease severity and clinical outcomes in patients with idiopathic granulomatous mastitis. J Clin Med 10: 2077, 2021.
33. Jiang L, Li X, Sun B, Ma T, Kong X and Yang Q: Clinicopathological features of granulomatous lobular mastitis and mammary duct ectasia. Oncol Lett 19: 840-848, 2020.
34. Schelfout K, Tjalma WA, Cooremans ID, Coeman DC, Colpaert CG and Buytaert PM: Observations of an idiopathic granulomatous mastitis. Eur J Obstet Gynecol Reprod Biol 97: 260-262, 2001.
35. Li SB, Xiong Y, Han XR, Liu ZY, Lv XL and Ning P: Pregnancy associated granulomatous mastitis: Clinical characteristics, management, and outcome. Breastfeed Med 16: 759-764, 2021.
36. Çetinkaya G, Kozan R, Emral AC and Tezel E: Granulomatous mastitis, watch and wait is a good option. Ir J Med Sci 190: 1117-1122, 2021.
37. Hurley K, Lacey N, O'Dwyer CA, Bergin DA, McElvaney OJ, O'Brien ME, McElvaney OF, Reeves EP and McElvaney NG: Alpha-1 antitrypsin augmentation therapy corrects accelerated neutrophil apoptosis in deficient individuals. J Immunol 193: 3978-3991, 2014.
38. Williams MS, McClintock AH, Bourassa L and Laya MB: Treatment of granulomatous mastitis: Is there a role for antibiotics? Eur J Breast Health 17: 239-246, 2021.
39. Co M, Cheng VCC, Wei J, Wong SCY, Chan SMS, Shek T and Kwong A: Idiopathic granulomatous mastitis: A 10-year study from a multicentre clinical database. Pathology 50: 742-747, 2018.
40. Uysal E, Soran A and Sezgin E; Granulomatous Mastitis Study Group: Factors related to recurrence of idiopathic granulomatous mastitis: What do we learn from a multicentre study? ANZ J Surg 88: 635-639, 2018.
41. Tang ELS, Ho CSB, Chan PMY, Chen JJC, Goh MH and Tan EY: The therapeutic dilemma of idiopathic granulomatous mastitis. Ann Acad Med Singap 50: 598-605, 2021.
42. Hu X, Fan Y, Li H, Zhou R, Zhao X, Sun Y and Zhang S: Impacts of cigarette smoking status on metabolomic and gut microbiota profile in male patients with coronary artery disease: A multi-omics study. Front Cardiovasc Med 8: 766739, 2021.
43. Kim SW, Kim HJ, Min K, Lee H, Lee SH, Kim S, Kim JS and Oh B: The relationship between smoking cigarettes and metabolic syndrome: A cross-sectional study with non-single residents of Seoul under 40 years old. PLoS One 16: e0256257, 2021.
44. Chen X, Zhang W, Yuan Q, Hu X, Xia T, Cao T, Jia H and Zhang L: A novel therapy for granulomatous lobular mastitis: Local heat therapy. Exp Ther Med 22: 1156, 2021.
45. Taylor GB, Paviour SD, Musaad S, Jones WO and Holland DJ: A clinicopathological review of 34 cases of inflammatory breast disease showing an association between corynebacteria infection and granulomatous mastitis. Pathology 35: 109-119, 2003.
46. Yu HJ, Deng H, Ma J, Huang SJ, Yang JM, Huang YF, Mu XP, Zhang L and Wang Q: Clinical metagenomic analysis of bacterial communities in breast abscesses of granulomatous mastitis. Int J Infect Dis 53: 30-33, 2016.
47. Bauer A, Hofmeyer S, Gere M, Nilsson K and Tot T: Granulomatous mastitis caused by Rickettsia species. Virchows Arch 479: 1091-1094, 2021.
48. Zhang X, Cong L, Xu D, Leng Q, Shi M and Zhou Y: AC092127.1-miR-451a-AE binding protein 2 signaling facilitates malignant properties of breast cancer. J Breast Cancer 24: 389-401, 2021.
49. Liu C, Pan A, Chen X, Tu J, Xia X and Sun L: MiR-5571-3p and miR-135b-5p, derived from analyses of microRNA profile sequencing, correlate with increased disease risk and activity of rheumatoid arthritis. Clin Rheumatol 38: 1753-1765, 2019.